

Coupling the immunomodulatory properties of the HDAC6 inhibitor ACY241 with Oxaliplatin promotes robust anti-tumor response in non-small cell lung cancer

Arup Bag^a, Andrew Schultz^a, Saloni Bhimani^a, Olya Stringfield^b, William Dominguez^c, Qianxing Mo^d, Ling Cen^d, and Dennis Adeegbe^a

^aDepartment of Immunology, H. Lee. Moffitt Cancer Center, Tampa, Florida, USA; ^bDepartment of Thoracic Oncology, H. Lee. Moffitt Cancer Center, Tampa, FL, USA; ^cSmall Animal Imaging Lab, H. Lee. Moffitt Cancer Center, Tampa, FL, USA; ^dDepartment of Biostatistics and Bioinformatics, H. Lee. Moffitt Cancer Center, Tampa, FL, USA

ABSTRACT

While HDAC inhibitors have shown promise in hematologic cancers, their efficacy remains limited in solid cancers. In the present study, we evaluated the immunomodulatory properties of the HDAC6 inhibitor, Citarinostat (ACY241) on lung tumor immune compartment and its therapeutic potential in combination with Oxaliplatin. As a single agent, ACY241 treatment promoted increased infiltration, activation, proliferation, and effector function of T cells in the tumors of lung adenocarcinoma-bearing mice. Furthermore, tumor-associated macrophages exhibited downregulated expression of inhibitory ligands in favor of increased MHC and co-stimulatory molecules in addition to higher expression of CCL4 that favored increased T cell numbers in the tumors. RNA-sequencing of tumor-associated T cells and macrophages after ACY241 treatment revealed significant genomic changes that is consistent with improved T cell viability, reduced inhibitory molecular signature, and enhancement of macrophage capacity for improved T cell priming. Finally, coupling these ACY241-mediated effects with the chemotherapy drug Oxaliplatin led to significantly enhanced tumor-associated T cell effector functionality in lung cancer-bearing mice and in patient-derived tumors. Collectively, our studies highlight the molecular underpinnings of the expansive immunomodulatory activity of ACY241 and supports its suitability as a partner agent in combination with rationally selected chemotherapy agents for therapeutic intervention in NSCLC.

ARTICLE HISTORY

Received 21 December 2021
Revised 27 January 2022
Accepted 10 February 2022

KEYWORDS

Non-small cell lung cancer; histone deacetylase inhibitor; immunomodulatory; chemotherapy; pre-clinical


Introduction

Non-small cell lung cancer (NSCLC) which accounts for over 80% of all lung cancers is a leading cause of cancer-related deaths worldwide. While immunotherapy leads to durable therapeutic responses in a subset of NSCLC patients,¹ there is still an unmet clinical need for drugs that could benefit a wider pool of patients. Histone deacetylase (HDAC) inhibitors are increasingly being evaluated in oncologic applications as promising therapeutic agents for cancer therapy in part due to their cytotoxic and cytostatic effects on tumor cells.^{2,3} The pan-HDAC inhibitors Panobinostat and Vorinostat are FDA-approved agents for multiple myeloma and cutaneous T-cell lymphoma, respectively.⁴⁻⁶ In recent years, research into the utility of these and other pan-HDAC inhibitors in solid tumors has increased considerably.^{2,3,7,8} However, due to potential toxicity concerns, more selective HDAC inhibitors are being increasingly considered as alternatives to pan-HDAC inhibitors based on expanding knowledge of the roles of various HDAC proteins in cancer biology. Among the selective HDAC inhibitors currently being explored are those targeting members of the class I^{1-3,8} and II^{4-7,9,10} HDACs which regulate various aspects of cancer biology including, proliferation, survival, metabolism, metastasis, autophagy, and apoptosis.^{8,9}

Despite their direct tumor cell toxicity, the effects of pan and isozyme selective HDAC inhibitors on immune cells are an important issue of consideration given the crucial contribution of immune cells to shaping the course of tumor progression. A number of HDAC inhibitors have been described to possess properties that have direct relevance to immune response in cancer. For example, Panobinostat promoted upregulation of PD-1 ligands while Trichostatin A and Panobinostat enhanced the expression of MHC class I and tumor-related antigens in melanoma to promote PD-1 therapy response and enhance tumor cell immunogenicity.¹⁰⁻¹³ HDAC inhibitors can also directly or indirectly regulate immune cells.¹⁴⁻¹⁶ In alignment with this notion, Romidepsin enhanced expression of T cell recruiting chemokines by tumor cells facilitating T cell infiltration into lung tumors in a mouse model of lung cancer.¹⁶ Understanding the nature and scope of immunomodulatory capabilities of HDAC inhibitors is no doubt paramount to their utility as suitable partner agents in novel combinatorial drug regimens. In this regard, the present study evaluated the effects of ACY241, an orally available HDAC6 inhibitor, which while structurally similar to Ricolinostat, is more potent with respect to its selectivity

CONTACT Dennis Adeegbe  Dennis.Adeegbe@moffitt.org  H. Lee Moffitt Cancer Center, 13131 USF Magnolia Drive, Tampa, FL 13131 USF +813-745-3112

The authors declare no potential conflicts of interest

 Supplemental data for this article can be accessed on the [publisher's website](#).

© 2022 The Author(s). Published with license by Taylor & Francis Group, LLC.

This is an Open Access article distributed under the terms of the Creative Commons Attribution-NonCommercial License (<http://creativecommons.org/licenses/by-nc/4.0/>), which permits unrestricted non-commercial use, distribution, and reproduction in any medium, provided the original work is properly cited.

for HDAC6 (IC50 of 2.6 nM versus 5 nM) in addition to having improved solubility properties.^{17,18} We investigated the spectrum of ACY241's effect on tumor-infiltrating T cells and macrophages in a pre-clinical mouse model of NSCLC with emphasis on molecular underpinnings of drug effect and its potential utility as a partner agent in a rationally selected combinatorial drug regimen for NSCLC therapy.

Material and methods

Mice, cell lines and tissues

All breeding and treatment experiments were performed with the approval of Moffitt Cancer Center Animal Care and Use Committee. Mice were maintained under specific-pathogen-free conditions in an AAALAC-accredited facility and in accordance with institutional guidelines for animal welfare. Genetically engineered mice *Kras*^{+/*LSL-G12D*}; *Trp53*^{L/L} (KP) have been previously described.¹⁹ For lung tumor induction, mice received 1×10^6 CFU of Cre-encoding adenovirus (Adeno-Cre) intranasally at 5–6 weeks of age. Tumor formation was evaluated by Magnetic Resonance Imaging (MRI) with BioSpec USR70/30 horizontal bore system (Bruker). Tumor burden was quantified from the MRI images with 3D Slicer software. Six weeks old C57BL/6 J (B6) mice were purchased from The Jackson laboratories. OT-I and OT-II mice were a kind gift from Drs. Filippo Veglia and Shari Pilon-Thomas, respectively, at Moffitt Cancer Center. B6 OVA 10103 F LT1 OVA-PGK, a KP lung cancer cell line that expresses CD4- and CD8-specific epitopes of Ovalbumin (OVA) was a kind gift from Dr. Tyler Jacks (MIT). Cell line was cultured in RPMI1640 supplemented with 10% FBS (Gemini), 1% penicillin/streptomycin and Glutamine (Gibco). Cell cultures were maintained at 37°C in a humid atmosphere containing 5% CO₂ and 95% air. Cell lines were routinely tested for Mycoplasma (every three months) and were authenticated (every six months) by STR authentication. De-identified patient tumor tissues were obtained under an IRB-approved protocol (IRB #00000971) from consented patients at the Moffitt Cancer Center.

In vivo treatment and cell transfer studies

After MRI-confirmation of tumors, mice with established tumors (150–200mm³) were randomly assigned to treatment groups. For short-term treatment studies involving genomic profiling by RNA-sequencing, KP mice were treated i.p. with ACY241 (25 mg/kg body weight) 3x/week for three weeks. Control mice received vehicle (5% DMSO in 10% 2-hydroxypropyl β -cyclodextrin). For long-term drug efficacy studies, ACY241 was administered 3x/week and Oxaliplatin (10 mg/kg body weight) was administered 1x/week i.p. in either the single agent or the combination groups for 6 weeks after which they were monitored until clinical endpoint. α -CCL4 antibody (clone W15194A, 50 μ g/mouse, i.p.) was administered 2x/week for 4 weeks. For mice with OVA-expressing lung tumors, B6 mice were implanted with B6 OVA 10103 F LT1 OVA-PGK tumor

cell line. After tumor establishment as documented by MRI, mice were randomly assigned into vehicle or ACY241 treatment groups. ACY241 or vehicle was administered 3x/week for 3 weeks after which tumors were harvested for flow cytometry and ImageStream analysis. T cells purified from the spleens of OT-I and OT-II T TCR transgenic mice were injected intravenously into B6 mice after inoculation with B6 OVA 10103 F LT1 OVA-PGK tumor cell line.

Multiparameter flow cytometry

Processing of tumor nodules into single-cell suspensions and immune profiling by flow cytometry have been previously described.²⁰ The gating strategy for FACS analyses is shown in supplementary figure 14. For acetylated α -tubulin staining, cytoplasmic expression was assessed using the BD Cytofix/Cytoperm Kit (BD Biosciences). For HDAC6 staining, this same kit was employed for cytoplasmic detection while the Ebioscience transcription buffer kit (ebioscience, Santa Clara, CA) was used for cytoplasmic and intracellular expression. Pre-incubation of cells permeabilized with the BD kit using unlabeled antibody was performed to block cytoplasmic HDAC6 (cold competition) prior to second staining with labeled antibody of the same clone which was carried out after permeabilization with Ebioscience kit in order to distinguish signals from cytoplasmic versus nuclear cellular locations.

Cell purifications and Ex vivo T cell activation assay

T cells from the spleen of OT-I and OT-II mice or lung tumors of treated KP mice were isolated from single-cell suspensions using CD90.2 Magnetic beads (Miltenyi) according to the manufacturer's protocol. For ex-vivo T cell activation, 1×10^6 T cells isolated from lung tumors were stimulated at 37°C with eBioscience™ Cell Stimulation Cocktail plus protein transport inhibitors (ThermoFisher Scientific) for 6 hours. Cells were washed and stained for intracellular cytokines using BD cytofix/cytoperm kit (BD Biosciences) according to the manufacturer's instructions at the end of the 6-hour culture. Briefly, cells were first stained for surface markers, including CD4, CD8, and CD3, followed by intracellular staining with fluorophore-conjugated antibodies against IL-2, TNF- α , CD107a, and IFN- γ , or isotype-matched antibodies after fixation and permeabilization. In all stained samples, dead cells were excluded using LIVE/DEAD Fixable Aqua Dead Cell Staining Kit (Invitrogen, Carlsbad, CA).

Antibodies

All antibodies used for flow cytometry analysis were purchased from BD Biosciences (San Jose, CA), Biolegend (San Diego, CA), Invitrogen (Carlsbad, CA), Novus Biologicals (Centennial, CO), or abcam (Waltham, MA) and are listed in supplementary table 2.

RNA-seq and data analysis

A total amount of 1 µg RNA per sample was used as input material for the RNA sample preparations the details of which are provided in Supplementary information. Sequencing libraries were generated using NEBNext® Ultra™ RNA Library Prep Kit for Illumina® (NEB, USA) following manufacturer's recommendations and index codes were added to attribute sequences to each sample. The library preparations were sequenced on an Illumina NextSeq 2000 platform and paired-end reads were generated. Raw data (reads) of FASTQ format were first processed to obtain clean reads by removing adapters, poly-N sequences and reads with low quality. The STAR aligner (v2.6.1) was then utilized to align the data to the mouse reference genome mm10, (Ensemble gene annotations). FeatureCounts (v1.5.0) was used to count the read numbers mapped of each gene and Reads Per Kilobase of exon model per Million mapped reads (RPKM) of each gene was calculated based on the length of the gene and reads count mapped to this gene.²¹ Differential expression analysis between two conditions/groups was performed using DESeq2 R package (v1.30.0). The resulting P values were adjusted using the Benjamini and Hochberg's approach for controlling the False Discovery Rate (FDR). Genes with an adjusted P value < .05 found by DESeq2 were assigned as differentially expressed. Gene set enrichment analysis was performed with GSEA (v4.1.0) and hallmark, Gene Ontology, and KEGG gene sets obtained from Molecular Signatures Database (v7.4). We also conducted pathway enrichment analysis utilizing the GeneGo MetaCore +MetaDrug™ tool (Thompson Reuters, version 6.31 build 68930). Triplicate samples were initially processed. However, vehicle sample 3 for T cells and ACY241 sample 2 for TAMs were deemed as low quality and were excluded from further analysis. The RNA sequencing data have been deposited in the NCBI GEO public data repository.

Patient tumor 2-D cultures

Fresh resected NSCLC patient tumors were gently dissociated mechanically in RPMI 1640 media containing 10 U/mL Collagenase D (Sigma Aldrich) and 25 µg/mL DNase I grade II (Sigma Aldrich) followed by incubation at 37°C for 30 minutes. Dissociated tissue was further digested using GentleMACS (Miltenyi) after which single cells were passed over a 100 µm filter. Tumor cell suspensions were co-cultured with autologous monocytes pulsed with tumor cell lysate in the presence of complete media supplemented with 40 IU/ml of IL-2 and 10 ng/ml of IL-15. ACY241 and Oxaliplatin were added at a concentration of 10 µg/ml while DMSO (0.05%) was added to control wells. For viability studies, cells were maintained in culture for 4 days after which immunofluorescent staining was performed to determine the viability of tumor and immune cells by first staining with LIVE/DEAD dye followed by antibodies against EpCAM and CD45. For assessment of effector capacity of tumor-associated T cells, tumor cultures were maintained in the presence or absence of each drug or combination for 36 hours after which cells were washed and re-stimulated with Cell Stimulation Cocktail plus protein transport inhibitors (ThermoFisher Scientific) for 6 hours prior to intracellular staining for TNF-α and IFN-γ.

ImageStream analysis

Subcutaneous tumors were developed using B6 OVA 10103 F LT1 OVA-PGK cell line and tumor-bearing mice were treated with either vehicle or ACY241 for 2 weeks after which tumors were resected from mice and processed into cell suspensions. Samples were subsequently stained with fluorophore-conjugated antibodies that included macrophage lineage markers as well as MHC class I and OVA₂₅₇₋₂₆₄-specific antibodies. Samples were acquired on the Amnis® ImageStream®X Mk II (Luminex) and analyzed with the IDEAS 6.2 software.

Statistical analysis

Data were analyzed using mean ± standard error of the mean (SEM). Unpaired two-tailed Student *t* test was used for comparisons between two groups using GraphPad Prism software. *P* values < .05 were considered statistically significant (*); *P* values < .01 are marked **, and *P* values < .001 are marked ***.

Results

ACY241 treatment supports increased infiltration, activation, and effector profile of T cells in the lung tumors of a pre-clinical mouse model of NSCLC

Although previous report demonstrated the immunomodulatory properties of Ricolinostat, an HDAC6 inhibitor in a murine model of NSCLC,²⁰ its effects on tumor-associated immune cells did not translate to improved anti-tumor response as a monotherapy. This promising result nonetheless led us to evaluate ACY241, a structurally similar compound with higher potency for HDAC6 inhibition and favorable solubility and safety profile.^{18,22} We postulated that ACY241 administration in our pre-clinical mouse model of NSCLC will likely be associated with broader effects in the tumor microenvironment in a manner that supports improved therapeutic efficacy. In this regard, we first evaluated the nature and scope of ACY241 effects on tumor-associated immune cell subsets using the *Kras* mutant, *p53*-deficient genetically engineered mouse model (GEMM) of NSCLC in which spontaneous lung adenocarcinoma development is driven by activating *Kras* mutation and concurrent *p53* deficiency (denoted KP).¹⁹

Upon tumor establishment (Supplementary Fig. S1) as confirmed by MRI, mice were treated with ACY241 or vehicle as controls (Figure 1a). We confirmed ACY241 activity in the tumor especially immune cells that are the focal point of our study by evaluating the acetylation of alpha-tubulin, which increases upon HDAC6 inhibition.^{23,24} Hyper-acetylation of α-tubulin was observed in tumor-associated T cells and macrophages upon ACY241 treatment (Supplementary Fig. S2). Analysis of resected tumors after treatment cessation by multi-parameter flow cytometry revealed an increase in the proportions of CD4+ Foxp3- and CD8+ effector T cells as well as NK cells in the tumors of ACY241-treated mice relative to the vehicle control group. In contrast, the proportions of CD4 + CD25hiFoxp3+ regulatory T cells (Tregs) was diminished (Figure 1b). Myeloid cell subsets including tumor-associated macrophages (TAMs), myeloid-derived suppressor cells

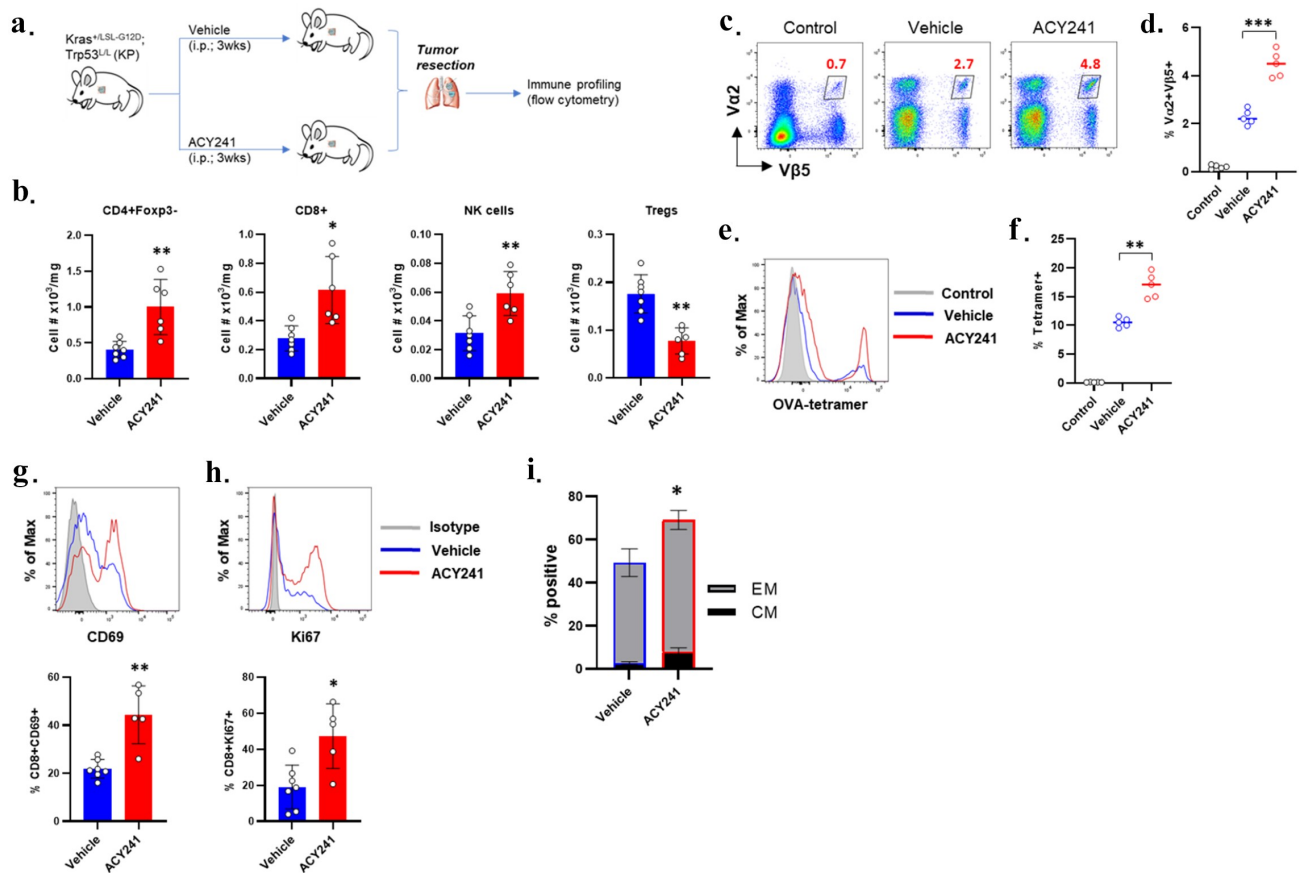


Figure 1. Increased infiltration and activation status of T cells in the tumors of ACY241-treated lung cancer-bearing mice. (a) Schematics of treatment and analysis of lung tumor-bearing KP mice. Lung tumor formation was induced in *Kras^{LSL-G12D}; Trp53^{L/L}* (KP) mice with intranasal administration of adeno-Cre. Mice with established tumors (150–200mm³) as confirmed by MRI were treated for three weeks with vehicle or ACY241 after which immune profiling was conducted by flow cytometry to assess the numbers and phenotype of immune cell subsets. (b) Proportion of CD4+ Foxp3-, CD8+ T cells, NK cells and Tregs (from left to right) within total viable cells per milligram of tumor. B6 mice orthotopically implanted with tumor cell line expressing CD4- and CD8-specific OVA epitopes were injected i.v. with a mixture of OT-I and OT-II TCR transgenic T cells and treated for 3 weeks with either vehicle or ACY241. Single cell suspensions from tumor nodules were analyzed for the proportions of OT-I or OT-II T cells. (c) Representative dot plots and (d) Summary for the frequency of tumor-infiltrating Va2+ Vβ5+ OT-I cells within gated CD8+ T cells. (e) Representative histograms and (f) Summary for OVA tetramer+ cells within gated tumor-infiltrating CD4+ T cells. Tumors from un-injected mice served as controls. (g, h) Representative histograms (top) and summary (bottom) of expression levels for (g) CD69 and (h) Ki67 on tumor-infiltrating CD8+ T cells in the spontaneous KP lung tumor model. (i) Percent of CD8+ T cells with an effector memory (EM) or central memory (CM) phenotype within tumor-infiltrating CD45+ CD3+ cells as determined by CD62L and CD44 staining in spontaneous KP tumors. Data are representative (c, e, g and h) or are mean \pm SEM (i) of 5–7 mice per group. * indicates p-value \leq 0.05, ** p-value \leq 0.01, *** p-value \leq 0.001.

(MDSC), and dendritic cells (DC) were, however, not significantly altered (Supplementary Fig. S3). Similar to the spontaneous KP tumor model, we found that when we orthotopically implanted wild-type B6 mice with tumor cell line expressing CD4- and CD8-specific Ovalbumin (OVA) epitopes and then adoptively transferred a mixture of OT-I and OT-II TCR transgenic T cells into these mice, there was an increase in the proportions of OVA-specific OT-I CD8+ (Figure 1c, d) and OT-II CD4+ (Figure 1e, f) T cells in the OVA-expressing lung tumors. Furthermore, phenotypic assessment of CD8+ and CD4+ Foxp3- T cells within the tumors of ACY241-treated KP GEMM showed that these cells exhibited enhanced activation status and proliferative profile evidenced by higher expression of CD69 and Ki67, respectively, compared to equivalent cells in the tumors of vehicle treated controls (Figure 1g, h, Supplementary Fig. S4A). In addition, these T cells harbored increased central (CD44+ CD62L+) and effector (CD44+ CD62L-) memory phenotypic subsets (Figure 1i and Supplementary Fig. S4B).

ACY241 treatment is associated with reduced dysfunctional phenotype and enhanced effector capacity of NSCLC-infiltrating CD8+ T cells

Given existing reports demonstrating that HDAC6 inhibition can alter the expression of inhibitory checkpoint molecules in melanoma patient T cells,²⁵ we evaluated the phenotype of lung adenocarcinoma-infiltrating T cells in our KP genetically engineered mouse model of NSCLC with particular focus on the expression pattern of inhibitory protein molecules as well as their effector function *ex vivo*. Flow cytometric assessment revealed that in the presence of ACY241 treatment, lung tumor-infiltrating CD8+ T cells expressed lower levels of the inhibitory receptors BTLA, PD-1, and CTLA-4 relative to the CD8+ T cells in the tumors of vehicle-injected control mice (Figure 2a-c, Supplementary Fig. S5A). As these inhibitory receptors contribute to T cell dysfunction,²⁶ their diminished expression under ACY241 treatment raises the possibility that they may be less functionally impaired compared to equivalent cells in untreated control tumors. Indeed, when stimulated ex-

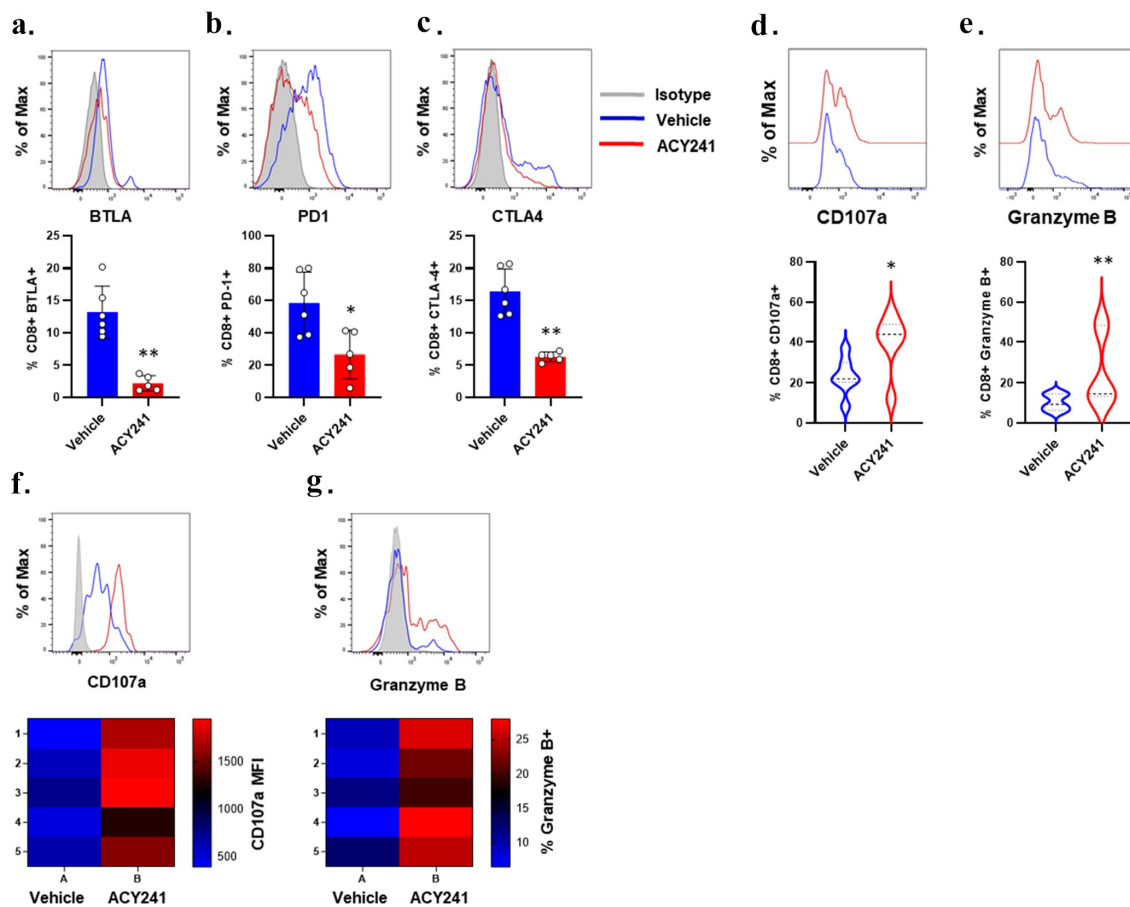


Figure 2. Reduced inhibitory receptor expression in tumor-infiltrating CD8 + T cells of ACY241-treated mice is accompanied by increased effector signature. Single cell suspensions generated from lung tumors of KP mice that were treated with vehicle or ACY241 were analyzed by flow cytometry to determine the phenotype of tumor-associated CD45+ CD3 + T cells. (a-c) Representative histograms (top) and summary (bottom) of expression levels for BTLA (a), PD-1 (b) and CTLA-4 (c) on tumor-infiltrating CD8 + T cell subset. T cells isolated from lung tumors of mice treated as indicated were stimulated for 6 hours with Cell Stimulation Cocktail plus protein transport inhibitor for subsequent intracellular cytokine staining. Representative histogram (top) and summary (bottom) for the expression of CD107a (d) or Granzyme B (e) on gated CD8 + T cells. B6 mice orthotopically implanted with KP tumor cell line expressing CD4-and CD8-specific OVA epitopes were injected i.v. with a mixture of OT-I and OT-II TCR transgenic T cells and treated for 3 weeks with either vehicle or ACY241. Single cell suspensions generated from the resected OVA-expressing lung tumors were similarly analyzed by flow cytometry. (f, g) Representative histograms (top) and corresponding heat maps (bottom) for the expression of CD107a (f) and Granzyme B (g) in Va2+ Vβ5+ OT-I cells within gated total tumor-infiltrating CD8 + T cells. Data in d and e (bottom) are mean ±SEM of 5–6 mice per group. * indicates p-value < 0.05, ** p-value < 0.01.

vivo, a higher proportion of tumor isolated CD8+ (Figure 2d, e) and CD4+ (Supplementary Fig. S5B, C) T cells expressed CD107a, an indicator of degranulation, and granzyme B, a cytotoxic granule associated with effector function under ACY241 treatment. Similarly, antigen-specific OT-I CD8 + T cells infiltrating orthotopic OVA-expressing lung tumors in mice that were injected with OT-I and OT-II T cells as described in Figure 1c-f showed significantly higher expression of CD107a and granzyme B when evaluated *ex-vivo* (Figure 2f, g). Collectively, these observations suggest that ACY241 promotes qualitative changes that is favorable to improved functionality of tumor-infiltrating T cells in NSCLC.

ACY241 treatment facilitates changes in tumor-associated macrophages that are conducive to enhanced antigenic stimulation of T cells

Besides the T cell compartment, we also interrogated the phenotype of myeloid cells, specifically tumor-associated macrophages (TAMs; CD11b+CD11c-Gr1-). Our analysis

revealed that both MHC class I and II molecules were substantially increased in TAMs present in the tumors of ACY241-treated mice relative to vehicle controls (Figure 3 a, b) suggesting that ACY241 may facilitate improved presentation of tumor antigens to T cells in the tumor bed. Consistent with this idea, we found that TAMs in the tumors of ACY241-treated mice displayed higher expression of CD8 + T cell-specific OVA epitope (OVA₂₅₆₋₂₆₄) in association with MHC class I (H-2Kb) in B6 mice bearing OVA-expressing tumors (Figure 3c, d, Supplementary Fig. S6A, B). We also observed a higher expression of this OVA antigenic peptide on the tumor cells in the ACY241 treatment condition (Supplementary Fig. S6C). In additional phenotypic analysis, we found that ACY241-exposed TAMs displayed increased levels of co-stimulatory molecules CD80, CD86, and CD40 while expressing reduced levels of the inhibitory ligands PD-L1 and PD-L2 (Figure 3e-i). These findings raise the possibility that ACY241 may tip the balance between activating and inhibitory signal availability to T cells in favor of the former in NSCLC.

ACY241 alters the transcriptional landscape of tumor-associated T cells and macrophages to reveal distinct genomic signatures accompanying its immunomodulatory effect

Although HDAC6 activity is often described in association with post-translational modification of its target proteins, such as α -tubulin, consistent with its largely cytoplasmic localization,^{27–29} increasing evidence support the idea that it likely has underappreciated transcriptional regulatory activity.^{30–32} Indeed, HDAC6 was present not only in the cytoplasm of tumor-associated immune cells of interest, specifically T cells and macrophages, but was also detected in the nucleus (Supplementary Fig. S7). To gain some insight into the mechanism of ACY241 action in the context of transcriptional regulation that likely accompanies its immunomodulatory effects, we performed RNA-sequencing of T cells and TAMs that were sorted from the tumors of vehicle versus ACY241-treated KP mice. Our analysis showed that only 213 genes were upregulated

in ACY241-exposed tumor-T cells whereas over 4,245 genes were downregulated (Log2 fold change greater than 1.5; Supplementary Table 1). There was generally no significant effect on T cell-associated canonical genes that are often involved in T cell signaling, activation, differentiation and/or function except for *IL33* and *Nfatc2ip* (Figure 4a, Supplementary Fig. S8A). However, genes involved in apoptosis including *Fas* and *Bax* were downregulated in ACY241-treated mice suggesting ACY241's potential for enhancement of T cell survival. Notably, several genes encoding inhibitory receptors or molecules involved in attenuation of T cell optimal function, such as *ctla4*, *vsir*, *tigit*, *Igals9*, and *Arg1*, were also downregulated in tumor-infiltrating T cells exposed to ACY241 (Figure 4a, Supplementary Fig. S8A). Gene set enrichment analysis (GSEA) further revealed that genes involved in apoptosis pathway and TGF-Beta signaling were downregulated in tumor-T cells upon ACY241 treatment (Figure 4b, c) suggesting that ACY241 activity may enhance survival and limit TGF-Beta inhibitory signaling.

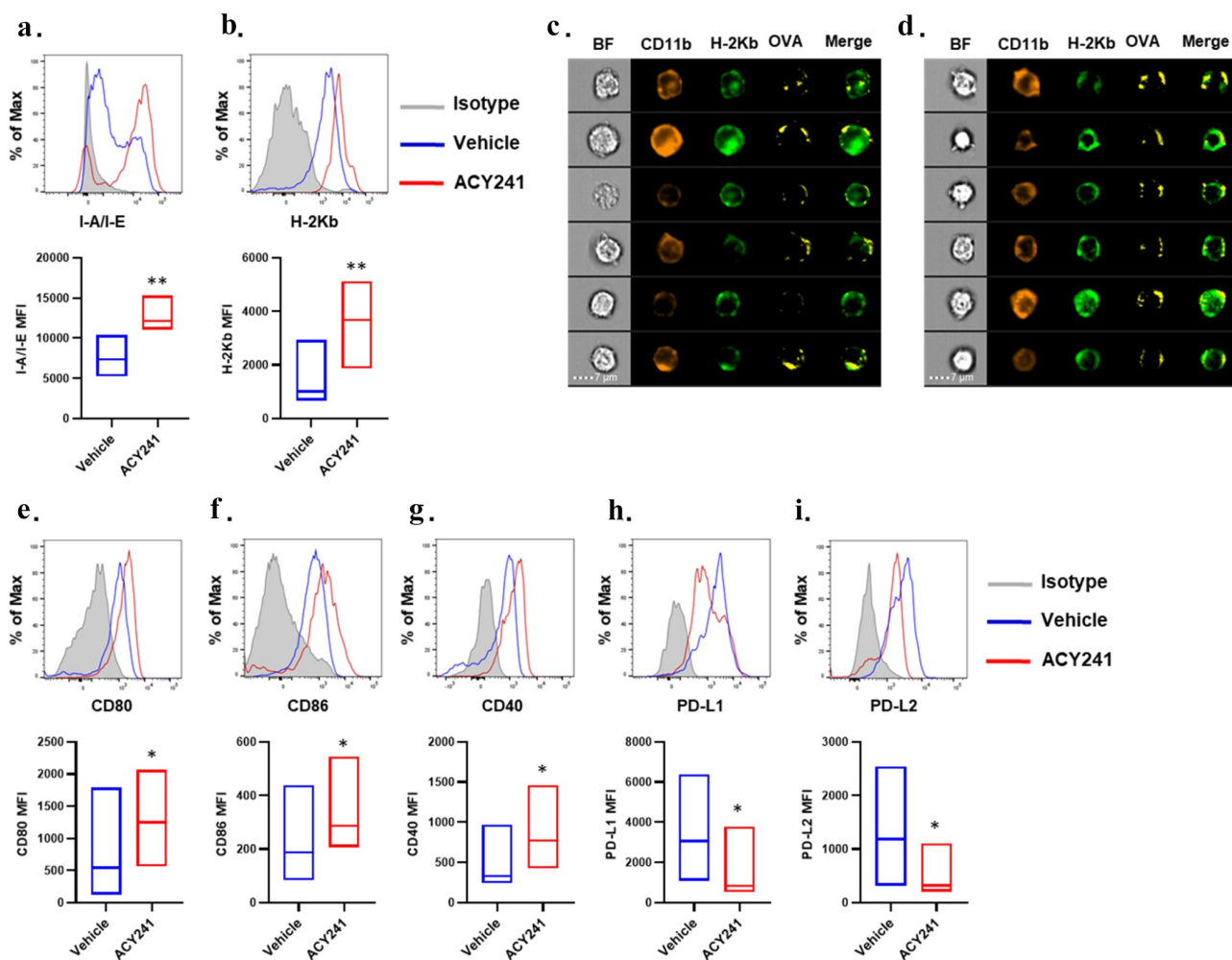


Figure 3. ACY241 potentiates phenotypic shift favoring upregulated expression of co-stimulatory molecules as well as tumor-expressed antigen over inhibitory ligands in tumor-associated macrophages. The phenotype of tumor-associated macrophages (TAMs; CD11b+CD11c-Gr-1-) in lung tumors of vehicle and ACY241-treated KP mice was evaluated by flow cytometry and imaging flow cytometry (ImageStream). Representative histograms (top) and summary (bottom) for the expression of (a) I-A/I-E (MHC class II), (b) H-2Kb (MHC class I). B6 mice were implanted with tumor cell line that expresses both CD4- and CD8-specific OVA epitopes. Mice were treated for 2 weeks with either vehicle or ACY241 after which tumor single cell suspensions were analyzed by imagestream. (c, d) Representative images for the expression of MHC class I H-2Kb and OVA₂₅₇₋₂₆₄ on CD11b+CD11c- macrophages in the tumors of vehicle (c) versus ACY241 (d) treated mice. (e-i) Representative histograms (top) and summary (bottom) for the expression of (e) CD80, (f) CD86, (g) CD40, (h) PD-L1, and (i) PD-L2 on TAMs in vehicle or ACY241-treated KP mice as determined from median fluorescent intensity (MFI). Data are representative or are mean \pm SEM of 5–7 mice per group. * indicates p-value $<$ 0.05, ** p-value $<$ 0.01.

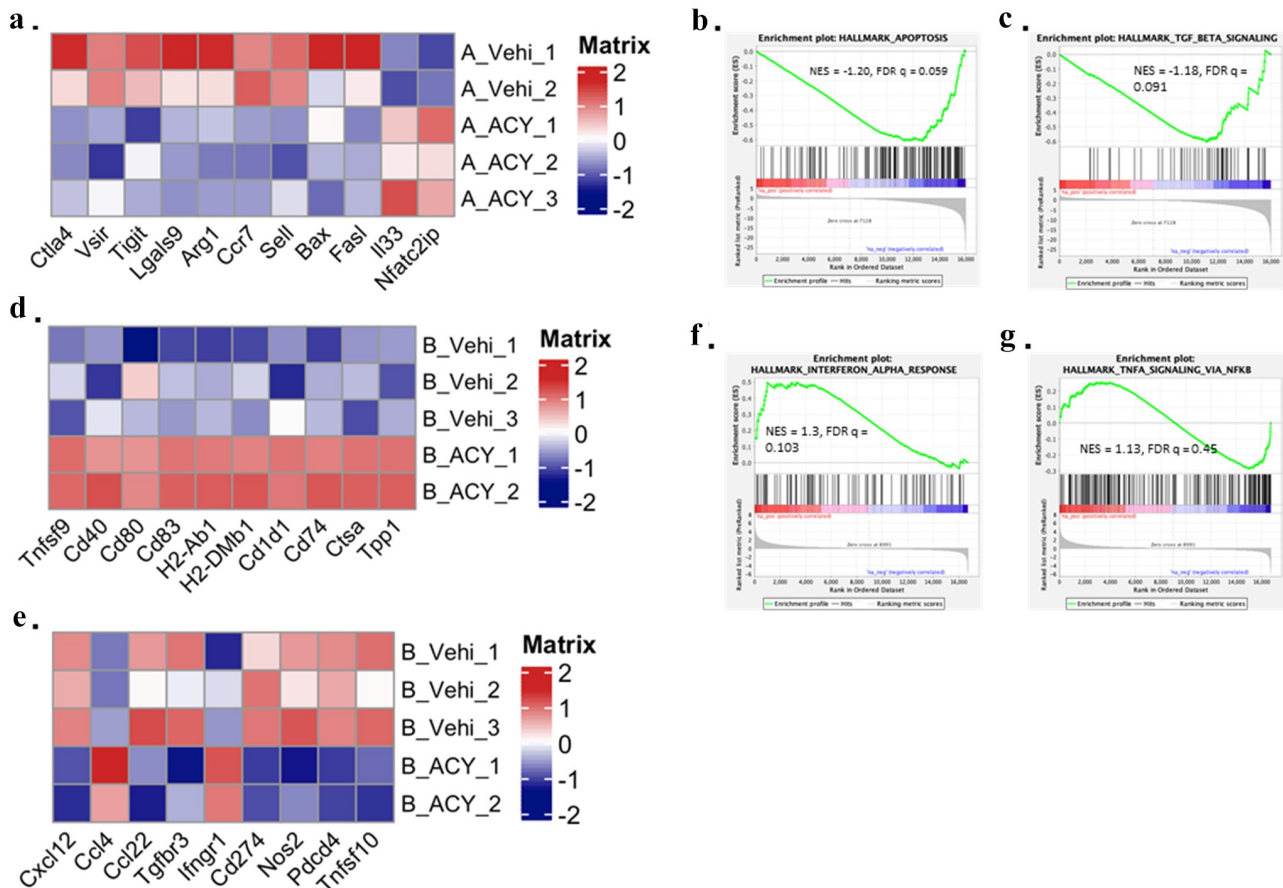


Figure 4. Transcriptomic analyses reveals genomic features that underlie the immunomodulatory activity of ACY241. CD45+ CD3+ Foxp3- T cells and CD45+ CD11b+CD11c-Gr-1- tumor-associated macrophages (TAMs) were concurrently sorted from lung tumors of vehicle and ACY241-treated KP mice for bulk RNA sequencing on the NextSeq500 Illumina platform. Data was analyzed by the R package Seurat analysis pipeline. (a) Heat map for immune-related differentially expressed genes ($\geq \log_2$ fold change at padj value 0.05) in tumor-T cells from ACY241-treated mice relative to vehicle controls. Gene set enrichment analysis (GSEA) was performed to identify pathways that are differentially enriched in tumor-T cells from ACY241-treated mice over vehicle. GSEA plot for (b) Apoptosis and (c) TGF-Beta signaling pathways. (d, e) Heat maps for immune-related differentially expressed genes ($\geq \log_2$ fold change at padj value 0.05) in TAMs from ACY241-treated mice relative to vehicle controls. (d) Expression pattern for indicated co-stimulatory, MHC, and related gene transcripts. (e) Expression pattern for indicated chemokines as well as indicated transcripts involved in attenuating T cell priming. (f, g) GSEA plots for (f) Interferon alpha response and (g) TNF-alpha signaling via NF- κ B as determined by enrichment scores for gene sets in indicated pathways.

Strikingly, in TAMs, 1,976 and 3,679 genes were up- or down-regulated, respectively, after ACY241 treatment relative to vehicle demonstrating a more profound effect of ACY241 on TAMs compared to T cells (Supplementary Table 1, Supplementary Fig. S8B). Among the most up-regulated genes are those encoding costimulatory molecules Tnfrsf9, Cd40, Cd80, Cd83; MHC proteins H2-Ab1, H2-DMb1, as well as related proteins Cd1d1, Cd74, Ctss, and Tpp1 (Figure 4d). A number of chemokine genes, such as *Cxcl12*, *Ccl4*, and *Ccl22*, were also differentially expressed (Figure 4e). Furthermore, among the most prominently downregulated gene transcripts are those whose protein derivatives play anti-inflammatory roles or function to attenuate T cell function. These include *Tgfb3*, *Cd274*, *Nos*, *Pcdcd4*, and *Tnfrsf10* (Figure 4e, Supplementary Fig. S8B). GSEA identified enrichment of genes that control Interferon alpha response and TNF-alpha signaling via NF- κ B as well as JAK/STAT signaling pathway (Figure 4f, g).

Oxaliplatin synergizes with ACY241 to support enhanced anti-tumor response and tumor-associated T cell effector function

The increased CCL4 expression in tumor-associated macrophages upon ACY241 treatment as revealed by RNA-sequencing prompted us to investigate whether this chemokine plays a key role in the recruitment of T cells into the tumor bed, culminating in the observed higher proportions. Consistent with increased CCL4 transcript in TAMs, there was more than 2-fold increase in the amount of CCL4 present in the supernatants of TAMs that were cultured in the presence of ACY241 for 24 hours relative to vehicle-exposed cells (Supplementary Fig. S9A). Furthermore, bronchoalveolar lavage (BAL) fluid obtained from tumor-bearing lungs of ACY241-treated mice had significantly higher levels of CCL4 compared to similar fluid from vehicle-treated mice (Supplementary Fig. S9B). To determine if neutralizing CCL4 impacts tumor growth kinetics and T cell proportions in the

tumors, we treated KP mice with established tumors (150–200mm³) with vehicle, ACY241 or ACY241 plus anti-CCL4 antibody. We found that the delayed tumor growth of mice treated with ACY241 was nearly abrogated in the presence of anti-CCL4 antibody treatment, an effect that was absent in mice co-treated with isotype control antibody (Figure 5a). Coincident with this finding, the increased tumor-infiltrating CD4⁺ Foxp3⁻ and CD8⁺ T cell numbers that accompanied ACY241 treatment was reversed under this anti-CCL4 /ACY241 co-administration (Supplementary Fig. S10A, B) implicating ACY241 enhancement of CCL4 as a recruitment mechanism for effector T cell infiltration into the tumor bed. Of note, CCR5, a receptor for CCL4 is expressed on a subset of tumor-infiltrating CD3⁺ Foxp3⁻ T cells but only marginally expressed on the Tregs (Supplementary Fig. S10C).

Next, we sought to determine whether the observed therapeutic effect of ACY241 as a monotherapy could be further amplified when combined with rationally selected partner agents. The chemotherapy drug Oxaliplatin has been reported to promote immunogenic cell death of

tumor cells.^{33–35} We reasoned that tumor-associated antigens arising from Oxaliplatin-supported tumor cell death is likely to be presented in the context of enhanced MHC expression and costimulatory signals if partnered with ACY241 and this may support enhanced anti-tumor T cell response. To this end, we treated lung tumor-bearing KP mice with ACY241 (3x/week) and/or Oxaliplatin (1x/week). Control mice received vehicle. Survival of mice treated with ACY241 alone mirrored those treated with Oxaliplatin alone although the former was slightly more efficacious in prolonging survival compared to vehicle-treated mice (MST 48 vs 41 vs 20). Administration of both agents concurrently achieved the most therapeutic outcome as mice treated with this combination survived much longer than those treated with either agent alone (MST 69) with some mice remaining alive past 80 days suggesting an additive effect from both drugs (Figure 5b). Consistent with these observations, tumor weight as measured after 6 weeks of treatment was significantly reduced in ACY241 or Oxaliplatin-

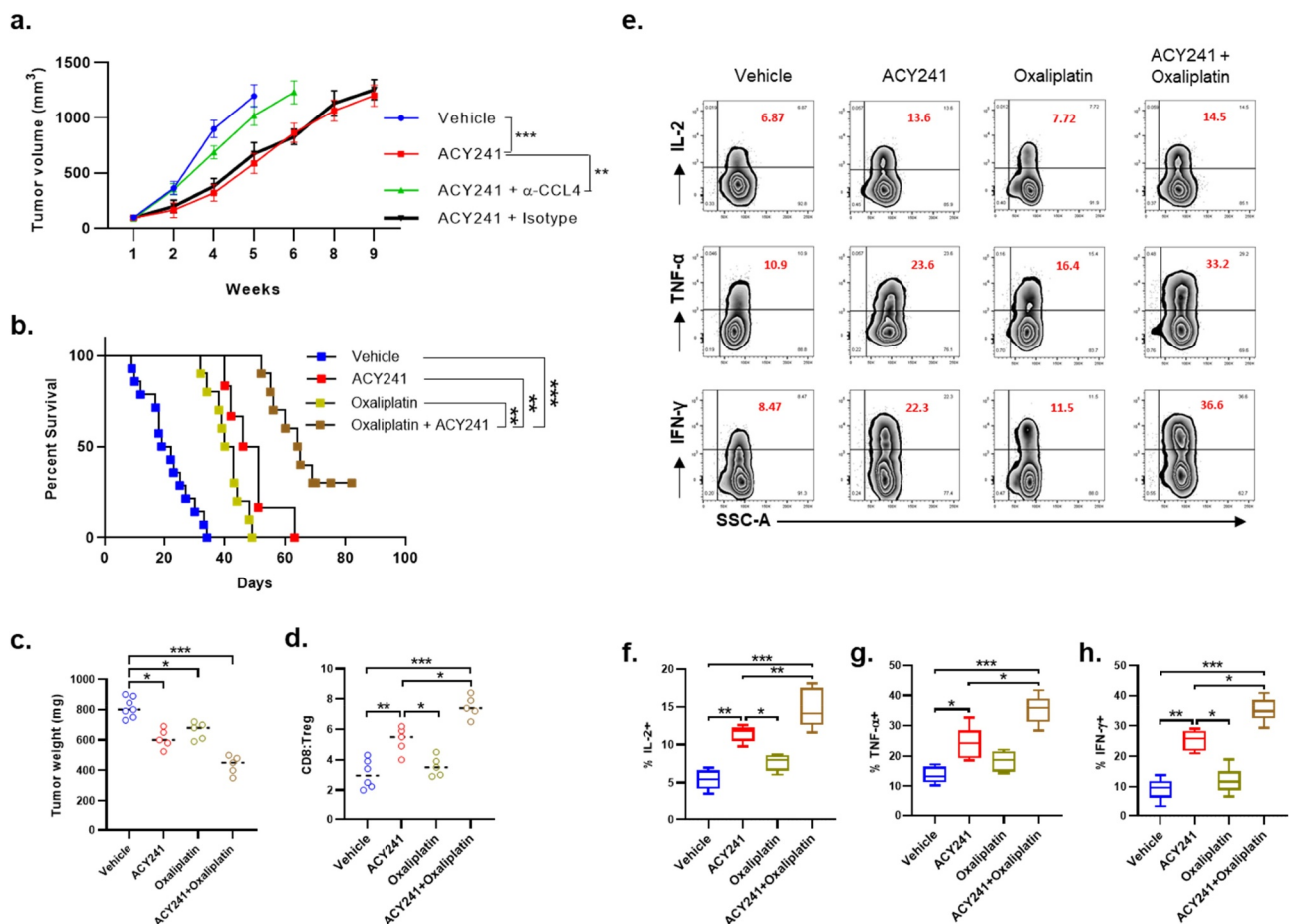


Figure 5. ACY241 coupled with Oxaliplatin significantly improves the survival of tumor-bearing mice. KP mice with established tumors (150–200mm³) received intraperitoneal injections of ACY241 (3X/week) and/or Oxaliplatin (1x/week) for 6 consecutive weeks. Mice receiving vehicle served as controls. One cohort was analyzed right after treatment cessation while a second cohort was monitored until clinical endpoints. (a) Kinetics of tumor growth in KP mice treated with vehicle or ACY241 with or without anti-CCL4 or isotype (control) antibodies. (b) Kinetics of survival for tumor-bearing mice that were treated as indicated and monitored long term. (c) Weight of tumor nodules in the lungs of treated mice analyzed right after 6-week treatment. Immune profiling was conducted by flow cytometry using tumor single cell suspensions to determine proportion of T cell subsets. (d) CD8⁺ T cells to Tregs (CD4⁺ CD25hiFoxp3⁺) ratio in tumors of mice in each treatment group. Tumor-infiltrating CD45⁺ CD3⁺ T cells were isolated from tumor cell suspensions and equivalent numbers stimulated for 6 hours with Cell Stimulation Cocktail plus protein transport inhibitor after which intracellular staining was conducted. Representative Zebra plot (e) or summary (f-h) for proportion of gated CD8⁺ T cells secreting IL-2 (e top, f), TNF- α (e middle, g), and IFN- γ (e bottom, h) under each treatment condition as indicated. Data are representative (e) or are mean \pm SEM (a, b, f-h) of 5–7 mice per group. * indicates p-value < 0.05, ** p-value < 0.01, *** p-value < 0.001.

treated mice relative to vehicle control, and this was further reduced in the presence of the two drugs. (Figure 5c). As myeloid-derived suppressor cells (MDSC) also contribute to dampening anti-tumor responses in lung cancer,^{36,37} we investigated whether agents that can deplete these cells as observed in our GEM model (Supplementary Fig. S11) such as Gemcitabine³⁸ might promote therapeutic outcomes when partnered with ACY241. Surprisingly, we found that Gemcitabine when combined with ACY241 did not promote any therapeutic benefit beyond what was associated with ACY241 alone (Supplementary Fig. S12). We also tested entinostat, a class I HDAC inhibitor which has been evaluated in patients with metastatic NSCLC³⁹ and found that unlike ACY241 monotherapy, it did not provide any survival benefit (Supplementary Fig. S12).

For mice analyzed at clinical endpoints in the ACY241/Oxaliplatin treatment cohorts, we found significantly increased CD8 + T cells:Treg ratio in the tumors of ACY241 + Oxaliplatin-treated mice that can be largely attributed to ACY241 effect (Figure 5d). Importantly, the capacity of these tumor-associated CD8 + T cells to produce IL-2, TNF- α , and IFN- γ upon *ex-vivo* stimulation was significantly increased in ACY241 and Oxaliplatin-treated mice compared to either agent alone (Figure 5e and f-h). Similar pattern was noted for the CD4 + T cells (Supplementary Fig. S13). Thus, ACY241 cooperated with Oxaliplatin to enhance polyfunctionality of tumor-associated T cells and promoted a durable anti-tumor response in our pre-clinical mouse model of NSCLC.

Combination of ACY241 and Oxaliplatin augments effector cytokine capacity of tumor-associated CD8 + T cells in *ex-vivo* patient tumor cultures

Given the therapeutic benefits of ACY241 and Oxaliplatin combination in the pre-clinical model as described above, we next investigated the effects of this drug combination on tumor-associated T cells in *ex-vivo* cultures of patient-derived tumor tissues. Interestingly, CD8 + T cells within tumor cultures exposed to ACY241 or Oxaliplatin for 36 hours showed enhanced ability to secrete TNF α and IFN γ compared to control cultures incubated with vehicle upon secondary TCR-independent stimulation. This outcome was even more profound in cultures containing both drugs (Figure 6a, b). To gauge the potential for clinical applicability of this combinatorial regimen, we investigated whether both agents together have deleterious effects on tumor-associated immune cells, which are important mediators of durable anti-tumor responses.⁴⁰ Thus, we evaluated the viability of tumor and immune cells in parallel cultures as described above and which were maintained for 4 days prior to analysis. While increased tumor cell death followed an increasing trend from ACY241 to Oxaliplatin to the combination, immune cells were largely unaffected in the presence of one or both drugs in this short-term culture (Figure 6c-f) suggesting that the combination of ACY241 and Oxaliplatin does not promote a significant toxic effect on tumor-associated immune cells.

Discussion

In hematologic cancers, both pan and selective HDAC inhibitors show promising therapeutic results.^{41,42} However, solid cancers have not met with the same level of success although emerging data is encouraging.^{2,13,16–18,22,43} In the present study, we evaluated ACY241, an HDAC6-selective inhibitor in a pre-clinical mouse model of NSCLC in order to determine its therapeutic potential in this disease by leveraging its identified immunomodulatory effects in new combinatorial drug regimen.

Our immunogenomic studies suggest that ACY241 has a broad effect on NSCLC-associated macrophages and T cells. Indeed, several genes involved in signaling, apoptosis, MHC assembly machinery, antigen presentation, co-inhibition, and co-stimulation were differentially altered in these cells upon ACY241 treatment relative to vehicle controls. The downregulation of gene sets involved in apoptosis pathway in tumor-associated T cells suggests that HDAC6 may play a critical role in regulating the survival of tumor-associated T cells. On the other hand, the upregulation of IFN- α and TNF- α signaling pathway-associated gene sets in macrophages raises the possibility that ACY241 may regulate macrophage activity in inflammatory immune responses. While HDAC6 activity is primarily cytosolic,^{27,28} it is readily detected in the nucleus of tumor-associated immune cell subsets as described. Our study supports the growing body of evidence that it likely exhibits significant transcriptional regulatory activity and it possibly interacts with other transcriptional factors, co-factors, and regulators to modulate transcriptional machinery associated with a number of genes.^{30–32} Indeed, HDAC6 interactions with Stat3 and the IL-10 gene promoter have been described.⁴⁴

Although only a fraction of tumor-associated T cells expressed CCR5 in our model, our findings suggest that the increased numbers of conventional T cells in the tumors of ACY241-treated mice may be mediated in part by CCL4-CCR5 chemokine signaling axis as this effect was abrogated with CCL4 neutralization. We postulate that ACY241-mediated enhanced production of CCL4 by macrophages is one potential mechanism promoting the increased recruitment of effector T cells into the tumor bed. Coupling this increased T cell presence with ACY241-mediated enhancement of co-stimulatory capability by macrophages provides an immunological recipe that likely facilitates improved effector T cell function as demonstrated in our studies.

While our findings suggest that ACY241 likely promotes recruitment, hence increased T cell numbers in the tumor microenvironment (TME), it remains a possibility that this increase is also due to clonal expansion of tumor-reactive T cells, a notion that is supported by our results from the OVA-specific T cell adoptive transfer studies in lung tumor-bearing mice in which OVA was expressed as a surrogate tumor antigen. We speculate that such clonal expansion may arise through an indirect effect whereby the composite of ACY241-associated increase in MHC expression, co-stimulatory molecules, and decrease in inhibitory ligands in APCs lowers the threshold for activation and priming of effector T cells with strong TCR affinities for tumor antigens, facilitating their expansion in the tumor.

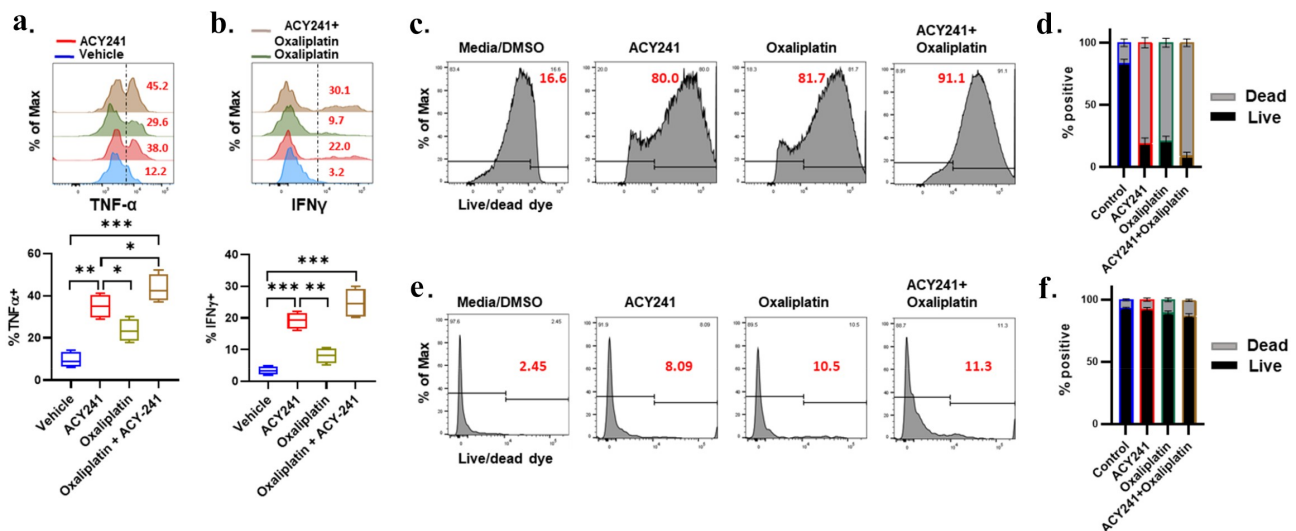


Figure 6. Combination of ACY241 and Oxaliplatin augments effector cytokine capacity of tumor-associated CD8 + T cells in *ex-vivo* patient tumor cultures. Freshly resected tumor tissues from non-small cell lung cancer patients were processed into single cell suspensions and co-cultured with autologous peripheral blood-derived monocytes pulsed with tumor cell lysate in complete media supplemented with 40IU/ml of IL-2 and 10 ng/ml of IL-15. ACY241 and Oxaliplatin were added at a concentration of 10ug/ml while DMSO in media was added to control cultures at similar concentration (0.01%) as the drug formulations. Cultures maintained for 36 hours were washed and re-stimulated with Cell Stimulation Cocktail plus protein transport inhibitors for 6 hours prior to intracellular cytokine staining. (a, b) Representative histograms (top) and summary (bottom) for the proportion of CD8 + T cells secreting TNFα (a) or IFNγ (b) within gated viable CD45+ CD3 + T cells. Cultures maintained for 96 hours were washed and stained with live/dead viability dye to determine live and dead cells in EpCAM+ tumor cells or CD45+ immune cells. (c, e) Representative histograms indicating live proportions of tumor (c) or immune (e) cells that are dead as determined by positive staining for the live/dead viability dye. (d, f) Summary for the proportion of live versus dead cells in EpCAM+ tumor (d) or CD45+ immune cells (f). Data are representative (a, b, c, e) or mean ± SEM (d, f) of 3 independent experiments. * indicates p-value < 0.05, ** p-value < 0.01, *** p-value < 0.001.

This is plausible as tumor-associated T cells under ACY241 treatment exhibited increased proliferative profile compared to vehicle-treated group. Future studies focused on analysis of the T cell receptor repertoire of tumor-infiltrating T cells in the presence or absence of ACY241 treatment could shed light on these possibilities.

Tumor antigen vaccinations have been explored as a modality for immunotherapy of cancer.^{45,46} While tumor-associated antigens that are immunogenic have not been fully elucidated in lung cancer, our findings that ACY241 promotes broad phenotypic changes in both tumor-infiltrating T cells and TAMs that in principle should promote enhanced antigen presentation and co-activation of T cells supports its suitability in tumor vaccination settings. Given the observation that tumor-expressed OVA antigenic epitopes associated with MHC class I molecules was not only higher on tumor macrophages upon ACY241 treatment but was also upregulated on tumor cells, it is likely that ACY241 promotes increased immunogenicity of lung adenocarcinoma cells.

Although its therapeutic effect was modest as a single agent in our studies, we speculate that ACY241 is likely to be a suitable rationally selected partner drug in novel combinatorial drug regimens where the other agent precipitates increased availability of tumor antigens through immunogenic tumor cell death. Our results from its combination with Oxaliplatin is in alignment with this idea. The relatively unremarkable outcome of ACY241 + Gemcitabine combination, however, may be explained by the latter's inability to evoke immunogenic cell death (ICD)⁴⁷ despite being able to induce expression of most ICD markers. Given the toxicity often associated with chemotherapy agents,^{48,49} it was somewhat

surprising to us that the combination of ACY241 and Oxaliplatin was well tolerated in the treated mice with no observable evidence of severe toxicity. Thus, this regimen appears to show a relatively safe profile at least in this pre-clinical mouse model. In support of this inference, tumor-associated leukocytes in patient tumor cultures did not show impaired viability in the presence of both agents *in vitro* unlike tumor cells. Thus, we opine that the combination of ACY241 and low-dose Oxaliplatin could be a potentially tolerable drug regimen for consideration in NSCLC therapy.

Although ACY241 has been tested in clinical trials in combination with anti-PD-1 or paclitaxel (NCT02635061, NCT02551185),⁵⁰ its therapeutic potential in NSCLC is still being explored. In the NCT02635061 clinical trial that tested the combination of ACY241 with anti-PD-1, patients with confirmed unresectable NSCLC for which nivolumab is clinically appropriate were enrolled. These patients must have had one line of prior therapy that was not an HDAC inhibitor, anti-PD-1, anti-PD-L1 or anti-CTLA-4 immunotherapy and must have progressed while on the prior therapy or have discontinued due to toxicity. With the reported responses observed in patients in the clinical trial,⁵⁰ and the robust activity as described in the present study, ACY241 could be a very promising non-prototypical immunotherapy agent if partnered with rationally selected drugs that cooperate, synergize, or amplify its immunostimulatory effects to a threshold that yields therapeutic outcomes. The increased effector functionality of patient tumor-associated CD8 + T cells exposed to ACY241 and Oxaliplatin *in vitro* supports the premise that Oxaliplatin is one such suitable partner agent for combination with ACY241. In this regard, further clinical assessment of this combination is worth exploring. Besides Oxaliplatin, our

studies suggest that ACY241 therapeutic potential will likely be maximized when partnered with other agents that capitalize on what it appears to do efficiently – enhance effector cell infiltration, support of macrophage-mediated T cell priming and lowering molecular brakes on T cells.

Abbreviations

cDNA Complementary DNA
 DC Dendritic cell
 FcR Fc receptor
 FDR False discovery rate
 GEMM Genetically engineered mouse model
 HDAC Histone deacetylase
 MDSC Myeloid-derived suppressor cell
 NK Natural killer
 NSCLC Non-small cell lung cancer
 OVA Ovalbumin
 TAM Tumor-associated macrophage
 TME Tumor microenvironment
 Treg Regulatory T-cells

Acknowledgments

We thank the Small animal imaging core facility for their contribution to MRI imaging of tumor-bearing mice and assistance with MRI image analysis, Neel Chaudhary for assistance with ImageStream analysis, the flow cytometry core for their support of sample acquisition, the tissue core for their provision of patient tissue samples, and the bioinformatics core for RNA-sequencing data analysis. Special thanks to Dr. Tyler Jacks for the generous gift of the B6 OVA 10103 F LT1 OVA-PGK tumor cell line.

Disclosure statement

No potential conflict of interest was reported by the author(s).

Funding

This work was supported by NCI 1K22CA222669-01 (to DA), American lung Association award ALA69-20210-02-01 (to D. A) and in part by the Flow Cytometry Core Facility at the Moffitt Cancer Center, an NCI designated Comprehensive Cancer Center (P30-CA076292).

Author contributions

AB, AS, SB, WD, DA: conducted experiments
 AB, AS, OS, QM, LC, DA: analyzed data.
 AB, QM, DA: interpreted data, edited the manuscript.
 AB, LC, DA: discussed data and manuscript.
 DA: designed research studies, discussed data sets, wrote the paper, supervised, and supported the research.

Availability of data and materials

The data generated and/or analyzed in this study are included in this published article (and its supplementary information files). The RNA-Seq data generated and/or reported in this study will be available in the Gene Expression Omnibus (GEO) repository upon acceptance for publication.

Ethics declarations

Ethics approval: All breeding and treatment studies were performed with the approval of Moffitt Cancer Center Animal Care and Use Committee. All animal work was conducted in accordance

with ARRIVE guidelines and in accordance with institutional guidelines for animal welfare.

Consent for publication:

Not applicable

References

- Doroshov DB, Sanmamed MF, Hastings K, Politi K, Rimm DL, Chen L, Melero I, Schalper KA, Herbst RS. Immunotherapy in non-small cell lung cancer: facts and hopes. *Clin Cancer Res.* 2019;25(15):4592–4602. doi:10.1158/1078-0432.CCR-18-1538.
- Lane AA, Chabner BA. Histone deacetylase inhibitors in cancer therapy. *J Clin Oncol.* 2009;27(32):5459–5468. doi:10.1200/JCO.2009.22.1291.
- Li Y, Seto E. HDACs and HDAC inhibitors in cancer development and therapy. *Cold Spring Harb Perspect Med.* 2016;6(10):a026831. doi:10.1101/cshperspect.a026831.
- Panobinostat approved for multiple myeloma. *Cancer Discov.* 2015; 5(5):OF4. doi:10.1158/2159-8290.CD-NB2015-040.
- Nooka AK, Kastiris E, Dimopoulos MA, Lonial S. Treatment options for relapsed and refractory multiple myeloma. *Blood.* 2015;125(20):3085–3099. doi:10.1182/blood-2014-11-568923.
- Mann BS, Johnson JR, Cohen MH, Justice R, Pazdur R. FDA approval summary: vorinostat for treatment of advanced primary cutaneous T-cell lymphoma. *Oncologist.* 2007;12(10):1247–1252. doi:10.1634/theoncologist.12-10-1247.
- Qiu T, Zhou L, Zhu W, Wang T, Wang J, Shu Y, Liu P. Effects of treatment with histone deacetylase inhibitors in solid tumors: a review based on 30 clinical trials. *Future Oncol.* 2013;9(2):255–269. doi:10.2217/fon.12.173.
- Ceccacci E, Minucci S. Inhibition of histone deacetylases in cancer therapy: lessons from leukaemia. *Br J Cancer.* 2016;114(6):605–611. doi:10.1038/bjc.2016.36.
- Li G, Tian Y, Zhu WG. The roles of histone deacetylases and their inhibitors in cancer therapy. *Front Cell Dev Biol.* 2020;8:576946. doi:10.3389/fcell.2020.576946.
- West AC, Christiansen AJ, Smyth MJ, Johnstone RW. The combination of histone deacetylase inhibitors with immune-stimulating antibodies has potent anti-cancer effects. *Oncoimmunology.* 2012;1(3):377–379. doi:10.4161/onci.18804.
- Khan AN, Gregorie CJ, Tomasi TB. Histone deacetylase inhibitors induce TAP, LMP, Tapasin genes and MHC class I antigen presentation by melanoma cells. *Cancer Immunol Immunother.* 2008;57(5):647–654. doi:10.1007/s00262-007-0402-4.
- Woods DM, Woan K, Cheng F, Wang H, Perez-Villarreal P, Lee C, Lienlaf M, Atadja, P, Seto E, Weber J, et al. The antimelanoma activity of the histone deacetylase inhibitor panobinostat (LBH589) is mediated by direct tumor cytotoxicity and increased tumor immunogenicity. *Melanoma Res.* 2013;23(5):341–348. doi:10.1097/CMR.0b013e328364c0ed.
- Woods DM, Sodre AL, Villagra A, Sarnaik A, Sotomayor EM, Weber J. HDAC inhibition upregulates PD-1 ligands in melanoma and augments Immunotherapy with PD-1 blockade. *Cancer Immunol Res.* 2015;3(12):1375–1385. doi:10.1158/2326-6066.CIR-15-0077-T.
- Armeanu S, Bitzer M, Lauer UM, Venturelli S, Pathil A, Krusch M, Kaiser S, Jobst J, Smirnow I, Wagner A, et al. Natural killer cell-mediated lysis of hepatoma cells via specific induction of NKG2D ligands by the histone deacetylase inhibitor sodium valproate. *Cancer Res.* 2005;65(14):6321–6329. doi:10.1158/0008-5472.CAN-04-4252.
- Licciardi PV, Karagiannis TC. Regulation of immune responses by histone deacetylase inhibitors. *ISRN Hematol.* 2012;2012:690901. doi:10.5402/2012/690901.
- Zheng H, Zhao W, Yan C, Watson CC, Massengill M, Xie M, Massengill C, Noyes DR, Martinez GV, Afzal R, et al. HDAC inhibitors enhance T-Cell chemokine expression and augment

- response to PD-1 immunotherapy in lung adenocarcinoma. *Clin Cancer Res.* 2016;22(16):4119–4132. doi:10.1158/1078-0432.CCR-15-2584.
17. Bae J, Hideshima T, Tai YT, Song Y, Richardson P, Raje N, Munshi NC, Anderson KC. Histone deacetylase (HDAC) inhibitor ACY241 enhances anti-tumor activities of antigen-specific central memory cytotoxic T lymphocytes against multiple myeloma and solid tumors. *Leukemia.* 2018;32(9):1932–1947. doi:10.1038/s41375-018-0062-8.
 18. Huang P, Almeciga-Pinto I, Jarpe M, van Duzer JH, Mazitschek R, Yang M, Jones SS, Quayle SN. Selective HDAC inhibition by ACY-241 enhances the activity of paclitaxel in solid tumor models. *Oncotarget.* 2017;8(2):2694–2707. doi:10.18632/oncotarget.13738.
 19. DuPage M, Dooley AL, Jacks T. Conditional mouse lung cancer models using adenoviral or lentiviral delivery of cre recombinase. *Nat Protoc.* 2009;4(7):1064–1072. doi:10.1038/nprot.2009.95.
 20. Adeegbe DO, Liu Y, Lizotte PH, Kamihara Y, Aref AR, Almonte C, Dries R, Li Y, Liu S, Wang X, et al. Synergistic immunostimulatory effects and therapeutic benefit of combined histone deacetylase and bromodomain inhibition in Non-Small cell lung cancer. *Cancer Discov.* 2017;7(8):852–867. doi:10.1158/2159-8290.CD-16-1020.
 21. Mortazavi A, Williams BA, McCue K, Schaeffer L, Wold B. Mapping and quantifying mammalian transcriptomes by RNA-Seq. *Nat Methods.* 2008;5(7):621–628. doi:10.1038/nmeth.1226.
 22. North BJ, Almeciga-Pinto I, Tamang D, Yang M, Jones SS, Quayle SN. Enhancement of pomalidomide anti-tumor response with ACY-241, a selective HDAC6 inhibitor. *PLoS One.* 2017;12(3):e0173507. doi:10.1371/journal.pone.0173507.
 23. Asthana J, Kapoor S, Mohan R, Panda D. Inhibition of HDAC6 deacetylase activity increases its binding with microtubules and suppresses microtubule dynamic instability in MCF-7 cells. *J Biol Chem.* 2013;288(31):22516–22526. doi:10.1074/jbc.M113.489328.
 24. Zhang Y, Li N, Caron C, Matthias G, Hess D, Khochbin S, Matthias P. HDAC-6 interacts with and deacetylates tubulin and microtubules in vivo. *EMBO J.* 2003;22(5):1168–1179. doi:10.1093/emboj/cdgl115.
 25. Laino AS, Betts BC, Veerapathran A, Dolgalev I, Sarnaik A, Quayle SN, Jones SS, Weber JS, Woods DM. HDAC6 selective inhibition of melanoma patient T-cells augments anti-tumor characteristics. *J Immunother Cancer.* 2019;7(1):33. doi:10.1186/s40425-019-0517-0.
 26. Thommen DS, Schumacher TN. T cell dysfunction in cancer. *Cancer Cell.* 2018;33(4):547–562. doi:10.1016/j.ccell.2018.03.012.
 27. Verdel A, Curtet S, Brocard MP, Rousseaux S, Lemerrier C, Yoshida M, Khochbin S. Active maintenance of mHDA2/mHDAC6 histone-deacetylase in the cytoplasm. *Curr Biol.* 2000;10(12):747–749. doi:10.1016/S0960-9822(00)00542-X.
 28. Bertos NR, Gilquin B, Chan GK, Yen TJ, Khochbin S, Yang XJ. Role of the tetradecapeptide repeat domain of human histone deacetylase 6 in cytoplasmic retention. *J Biol Chem.* 2004;279(46):48246–48254. doi:10.1074/jbc.M408583200.
 29. Boyault C, Sadoul K, Pabion M, Khochbin S. HDAC6, at the crossroads between cytoskeleton and cell signaling by acetylation and ubiquitination. *Oncogene.* 2007;26(37):5468–5476. doi:10.1038/sj.onc.1210614.
 30. Westendorf JJ, Zaidi SK, Cascino JE, Kahler R, van Wijnen AJ, Lian JB, Yoshida M, Stein GS, Li X. Runx2 (Cbfa1, AML-3) interacts with histone deacetylase 6 and represses the p21(CIP1/WAF1) promoter. *Mol Cell Biol.* 2002;22(22):7982–7992. doi:10.1128/MCB.22.22.7982-7992.2002.
 31. Zhang W, Kone BC. NF-kappaB inhibits transcription of the H (+)-K(+)-ATPase alpha(2)-subunit gene: role of histone deacetylases. *Am J Physiol Renal Physiol.* 2002;283(5):F904–11. doi:10.1152/ajprenal.00156.2002.
 32. Fernandes I, Bastien Y, Wai T, Nygard K, Lin R, Cormier O, Lee HS, Eng F, Bertos NR, Pelletier N, et al. Ligand-dependent nuclear receptor corepressor LCoR functions by histone deacetylase-dependent and -independent mechanisms. *Mol Cell.* 2003;11(1):139–150. doi:10.1016/S1097-2765(03)00014-5.
 33. Wang YJ, Fletcher R, Yu J, Zhang L. Immunogenic effects of chemotherapy-induced tumor cell death. *Genes Dis.* 2018;5(3):194–203. doi:10.1016/j.gendis.2018.05.003.
 34. Tesniere A, Schlemmer F, Boige V, Kepp O, Martins I, Ghiringhelli F, Aymeric L, Michaud M, Apetoh L, Barault L, et al. Immunogenic death of colon cancer cells treated with oxaliplatin. *Oncogene.* 2010;29(4):482–491. doi:10.1038/onc.2009.356.
 35. Shalpour S, Font-Burgada J, Di Caro G, Zhong Z, Sanchez-Lopez E, Dhar D, Willimsky G, Ammirante M, Strasner A, Hansel DE, et al. Immunosuppressive plasma cells impede T-cell-dependent immunogenic chemotherapy. *Nature.* 2015;521(7550):94–98. doi:10.1038/nature14395.
 36. Huang A, Zhang B, Wang B, Zhang F, Fan KX, Guo YJ. Increased CD14(+)/HLA-DR (-/low) myeloid-derived suppressor cells correlate with extrathoracic metastasis and poor response to chemotherapy in non-small cell lung cancer patients. *Cancer Immunol Immunother.* 2013;62(9):1439–1451. doi:10.1007/s00262-013-1450-6.
 37. Ortiz ML, Lu L, Ramachandran I, Gabrilovich DI. Myeloid-derived suppressor cells in the development of lung cancer. *Cancer Immunol Res.* 2014;2(1):50–58. doi:10.1158/2326-6066.CIR-13-0129.
 38. Sawant A, Schafer CC, Jin TH, Zmijewski J, Tse HM, Roth J, Sun Z, Siegal GP, Thannickal VJ, Grant SC, et al. Enhancement of anti-tumor immunity in lung cancer by targeting myeloid-derived suppressor cell pathways. *Cancer Res.* 2013;73(22):6609–6620. doi:10.1158/0008-5472.CAN-13-0987.
 39. Hellmann MD, Janne PA,OPYrchal M, Hafez N, Raez LE, Gabrilovich DI, Wang F, Trepel JB, Lee MJ, Yuno A, et al. Entinostat plus pembrolizumab in patients with metastatic NSCLC previously treated with Anti-PD-(L)1 therapy. *Clin Cancer Res.* 2021;27(4):1019–1028. doi:10.1158/1078-0432.CCR-20-3305.
 40. Fridman WH, Zitvogel L, Sautes-Fridman C, Kroemer G. The immune contexture in cancer prognosis and treatment. *Nat Rev Clin Oncol.* 2017;14(12):717–734. doi:10.1038/nrclinonc.2017.101.
 41. Chen IC, Sethy B, Liou JP. Recent update of HDAC inhibitors in lymphoma. *Front Cell Dev Biol.* 2020;8:576391. doi:10.3389/fcell.2020.576391.
 42. Pride DA, Summers AR. The emergence of specific HDAC inhibitors and their clinical efficacy in the treatment of hematologic malignancies and breast cancer. *Int J Mol Biol Open Access.* 2018;3(5):203–209. doi:10.15406/ijmboa.2018.03.00078.
 43. West AC, Johnstone RW. New and emerging HDAC inhibitors for cancer treatment. *J Clin Invest.* 2014;124(1):30–39. doi:10.1172/JCI69738.
 44. Cheng F, Lienlaf M, Wang HW, Perez-Villarrol P, Lee C, Woan K, Rock-Klotz J, Sahakian E, Woods D, Pinilla-Ibarz J, et al. A novel role for histone deacetylase 6 in the regulation of the tolerogenic STAT3/IL-10 pathway in APCs. *J Immunol.* 2014;193(6):2850–2862. doi:10.4049/jimmunol.1302778.
 45. Peng M, Mo Y, Wang Y, Wu P, Zhang Y, Xiong F, Guo C, Wu X, Li Y, Li X, et al. Neoantigen vaccine: an emerging tumor immunotherapy. *Mol Cancer.* 2019;18(1):128. doi:10.1186/s12943-019-1055-6.
 46. Gupta RG, Li F, Roszik J, Lizee G. Exploiting tumor neoantigens to target cancer evolution: current challenges and promising therapeutic approaches. *Cancer Discov.* 2021;11(5):1024–1039. doi:10.1158/2159-8290.CD-20-1575.
 47. Hayashi K, Nikolos F, Lee YC, Jain A, Tsouko E, Gao H, Kasabyan A, Leung HE, Osipov A, Jung SY, et al. Tipping the immunostimulatory and inhibitory DAMP balance to harness immunogenic cell death. *Nat Commun.* 2020;11(1):6299. doi:10.1038/s41467-020-19970-9.
 48. Hoff PM, Saad ED, Costa F, Coutinho AK, Caponero R, Prolla G, Gansl RC. Literature review and practical aspects on the management of oxaliplatin-associated toxicity. *Clin Colorectal Cancer.* 2012;11(2):93–100. doi:10.1016/j.clcc.2011.10.004.
 49. Mitchell EP. Gastrointestinal toxicity of chemotherapeutic agents. *Semin Oncol.* 2006;33(1):106–120. doi:10.1053/j.seminoncol.2005.12.001.
 50. Awad MM, Le Bruchec Y, Lu B, Ye J, Miller J, Lizotte PH, Cavanaugh ME, Rode AJ, Dumitru CD, Spira A. Selective histone deacetylase inhibitor ACY-241 (citarinostat) plus nivolumab in advanced Non-Small cell lung cancer: results from a phase Ib study. *Front Oncol.* 2021;11:696512. doi:10.3389/fonc.2021.696512.